

Article

# New Insights on Gene by Environmental Effects of Drugs of Abuse in Animal Models Using GeneNetwork

Alisha Chunduri <sup>1</sup> , Pamela M. Watson <sup>2</sup>  and David G. Ashbrook <sup>2,\*</sup> 

<sup>1</sup> Department of Biotechnology, Chaitanya Bharathi Institute of Technology, Hyderabad 500075, India; msd.alisha07@gmail.com

<sup>2</sup> Department of Genetics, Genomics, and Informatics, University of Tennessee Health Science Center, Memphis, TN 38163, USA; pwatso16@uthsc.edu

\* Correspondence: dashbrook@uthsc.edu

**Abstract:** Gene-by-environment interactions are important for all facets of biology, especially behaviour. Families of isogenic strains of mice, such as the BXD strains, are excellently placed to study these interactions, as the same genome can be tested in multiple environments. BXD strains are recombinant inbred mouse strains derived from crossing two inbred strains—C57BL/6J and DBA/2J mice. Many reproducible genotypes can be leveraged, and old data can be reanalysed with new tools to produce novel insights. We obtained drug and behavioural phenotypes from Philip et al. Genes, Brain and Behaviour 2010, and reanalysed their data with new genotypes from sequencing, as well as new models (Genome-wide Efficient Mixed Model Association (GEMMA) and R/qt12). We discovered QTLs on chromosomes 3, 5, 9, 11, and 14, not found in the original study. We reduced the candidate genes based on their ability to alter gene expression or protein function. Candidate genes included *Slitrk6* and *Cdk14*. *Slitrk6*, in a Chromosome14 QTL for locomotion, was found to be part of a co-expression network involved in voluntary movement and associated with neuropsychiatric phenotypes. *Cdk14*, one of only three genes in a Chromosome5 QTL, is associated with handling induced convulsions after ethanol treatment, that is regulated by the anticonvulsant drug valproic acid. By using families of isogenic strains, we can reanalyse data to discover novel candidate genes involved in response to drugs of abuse.

**Keywords:** addiction; human genetics; systems genetics; gene expression; bioinformatics; cross-species analysis; animal models; genomics; genetic mapping



**Citation:** Chunduri, A.; Watson, P.M.; Ashbrook, D.G. New Insights on Gene by Environmental Effects of Drugs of Abuse in Animal Models Using GeneNetwork. *Genes* **2022**, *13*, 614. <https://doi.org/10.3390/genes13040614>

Academic Editor: Jason Bubier

Received: 2 February 2022

Accepted: 7 March 2022

Published: 29 March 2022

**Publisher's Note:** MDPI stays neutral with regard to jurisdictional claims in published maps and institutional affiliations.



**Copyright:** © 2022 by the authors. Licensee MDPI, Basel, Switzerland. This article is an open access article distributed under the terms and conditions of the Creative Commons Attribution (CC BY) license (<https://creativecommons.org/licenses/by/4.0/>).

## 1. Introduction

Two of the biggest problems in analyses of biomedical data are irretrievability and irreproducibility. Biomedical data is often lost as soon as it is published, locked within a forgotten hard drive, or siloed in a little-used format on a lab's website. There are many efforts to make data publicly accessible and retrievable, such as the FAIR Principles (findability, accessibility, interoperability, and reusability) [1], and these allow the combined analysis of many datasets and reanalysis using new tools. There is still the problem of irreproducible datasets: for example, if a sample from a particular outbred cohort is found to be an outlier during data analysis, there is no way to go back to that genotype and remeasure the phenotype. Nor can new phenotypes be measured in the same individuals within the same environments later as new tools emerge. The genotype refers to all genotype states across the organism. Different strains in the BXD family might share the same genotype at a specific location, but the different strains are different genotypes. Families of isogenic strains solve this problem, allowing for reproducible genotypes that can be sampled many times, under many environmental conditions, leading to so-called experimental precision medicine [2]. This means that a genotype sampled 30 years ago in a different country can be replicated now, in any lab, with any environmental variable

of interest, using any technique. The GeneNetwork.org (<http://www.genenetwork.org/>, accessed on 2 February 2022) website allows this combination of FAIR data and reproducible genomes, meaning that research teams can now go back to previous datasets and reanalyse them with new data and new tools. Every new dataset adds exponentially to the number of possible connections. In this paper, we will reanalyse drug and addiction related data from over a decade ago, using new genotypes for the BXD family of murine strains, as well as new statistical tools, showing that we can identify new quantitative trait loci (QTLs), resulting in highly plausible candidate genes.

Quantitative trait locus (QTL) mapping has been carried out in numerous species to associate regions of the genome to phenotypes even before the structure of the genome was well understood (e.g., [3]). Rodents, especially mice, have been the species most prominently used for biomedically relevant traits. Amongst these, the BXD family of recombinant inbred (RI) strains derived from crossing two inbred strains—C57BL/6J and DBA/2J mice—have been extensively used for almost 50 years in fields such as neuropharmacology [4–6], immunology [7–13], behaviour [13–21], aging [21–29], neurodegeneration [30–33], and gut microbiome–host interactions [34].

The development of the BXD panel was started by Benjamin A. Taylor by inbreeding the progeny of female C57BL/6J and male DBA/2J strains, for the purpose of mapping Mendelian traits [35]. This led to the original 32 BXD strains, which now carry the suffix ‘TyJ’ (Taylor to Jackson Laboratory). To increase the power and precision of QTL mapping, the number of strains has been expanded [36], including through advanced intercross [37], to a total of 140 extant strains [2], making this resource the largest family of murine isogenic strains. Phenotypes in the BXD have been measured under many conditions, allowing for the identification of gene-by-environment interactions. Understanding these interactions can potentially help in the discovery of complex therapeutic solutions and are a vital part of the development of precision medicine.

GeneNetwork.org is a tool for quantitative genetics that started in 2001 as WebQTL [38]. It evolved from analyses of forward genetics in the BXD mouse family, to phenome-wide association studies and reverse genetics in a variety of species. Although GeneNetwork.org contains data for many species and populations, it most prominently contains data for the BXD family. Over 10,000 “classical” phenotypes, measured under a variety of environmental conditions and over 100 ‘omics datasets, are available on GeneNetwork.org for the BXD family. GeneNetwork.org and the BXD RI population are therefore a powerful tool for systems genetics and experimental precision medicine. The great advantage of inbred lines, with stable genotypes that can be resampled is that data can be reused and reanalysed over time, as tools improve. From the very start of the genome sequencing revolution, when loci were first mapped to causative genes, new tools and a greater understanding of the genome have allowed us to go back to old data and gain new insight.

In this study, we will demonstrate how new biological insight into drugs of abuse can be gained by reanalysing data in the BXD family, using improved genotypes from sequencing, and new mapping methods (linear mixed models). Using this method, we have discovered new QTLs and candidate genes for behavioural phenotypes associated with the predisposition of drug- and behaviour-related traits obtained from Philip et al. 2010 [39].

## 2. Materials and Methods

### 2.1. Phenotype Data

The traits used for analysis in this study were acquired by Philip and team and published in 2010 [39]. All datasets from this publication are freely available on GeneNetwork.org, and were obtained from the BXD published phenotypes ([http://gn1.genenetwork.org/webqtl/main.py?FormID=sharinginfo&GN\\_AccessionId=602&InfoPageName=BXDPublish](http://gn1.genenetwork.org/webqtl/main.py?FormID=sharinginfo&GN_AccessionId=602&InfoPageName=BXDPublish), accessed on 2 February 2022). The original study aimed to determine the influence of genes in response to the environment and the plausibility of similar interactions with drug-related attributes including response to and withdrawal from cocaine, 3,4-methylenedioxymethamphetamine, morphine, and ethanol and the correlation to phenotypic traits including anxiety, locomotion,

stress sensitivity, and pain sensitivity. Complex phenotyping batteries consisting of diverse behavioural assays were employed on the RI strains, and multivariate analyses were performed using GeneNetwork.org. An interplay between environmental factors, drug-induced neural changes, and genetic factors underlies the predisposition of an individual to addiction. In this study, a total of 762 traits were analysed (Supplementary Table S1) using new genotypes and linear mixed model (LMM) based mapping software, to identify novel candidate genes and gene-by-treatment interactions. However, we did not include morphine related traits, as these are being actively studied by others. Of the then extant population of 79 strains [7], Philip's study used approximately 70 strains to measure the traits.

## 2.2. New Genotypes from Sequencing

A total of 152 BXD strains have now been sequenced using linked-read technologies, and new genotypes for all 152 BXD strains have been produced from this (European Nucleotide Archive project PRJEB45429). Variants were chosen to define the start and end of each haplotype block, and variant positions from the previously published genotypes were kept allowing maximum back compatibility with previous publications.

## 2.3. Genome-Wide Efficient Mixed Model Association (GEMMA), Kinship within the BXD Strains, and QTL Mapping

The BXD family has been produced in several 'epochs' across 40 years, using both standard F2 recombinant inbred methods as well as advanced intercross recombinant inbred methods [2]. This has led to both expected and unexpected kinship between BXD strains. This kinship between strains can lead to bias, as it breaks the expectations of previously used methods, such as the Haley–Knott mapping algorithm that was used in the original study. Updated linear mixed models including R/qt2 (qt2 analysis using R software) and Genome-wide Efficient Mixed Model Association (GEMMA), which is accessible in GeneNetwork.org, have been used for this study as they allow correction for kinship, as well as other cofactors if needed.

An analysis of 762 traits taken from Philip et al. study was carried out using the GEMMA mapping tool with the genotypes from sequencing, a minor allele frequency (MAF) of 0.05, and utilizing the Leave One Chromosome Out (LOCO) method. This computation provides a  $-\log(p)$  value between each marker and the phenotype. We used a  $-\log(p) > 4$ , as significant. However, since permutations of the GEMMA algorithm are not currently available in GeneNetwork.org, we confirmed the significance of these QTL using the linear mixed model tool within R/qt2 [40], with 5000 permutations of the data.

## 2.4. Identification of Novel QTLs

Two methods were used to identify significant QTLs. Firstly, traits with an adjusted  $p < 0.05$  using permutation in R/qt2 (described above) were investigated at length, as these are significant after empirical correction. The second method used was to take advantage of independent traits which share QTL at the same location with suggestive  $p$ -values ( $p < 0.63$ ). This  $p < 0.63$  equates to one false positive per genome scan. However, the likelihood of any chromosome having a QTL on it is approximately 1 in 20 (i.e.,  $p < 0.05$ ) due to 20 chromosomes in mice. The likelihood of two independent traits sharing the same QTL location by chance is therefore much lower than  $p < 0.05$ . Traits were referred to as independent if they were carried out in separate groups of animals (e.g., males and females), or if the traits were measured at independent timepoints (e.g., at 10 min after treatment and 60 min after treatment).

## 2.5. QTL Confidence Intervals

A 1.5 LOD (logarithm of the odds) or 1.5  $-\log(p)$  drop [41] was used to determine the QTL confidence interval for each statistically significant trait (in our case of a two-parent population LOD and  $-\log(p)$  are approximately equal). Therefore, for each of the QTL above (Supplementary Table S2), we were able to generate a list of genes within this

confidence interval. Genes were called within the QTL interval using the GeneNetwork.org QTL mapping tool, which provides protein coding genes, non-coding genes, and predicted gene models.

### 2.6. *Cis-eQTL Mapping*

A *cis-eQTL* indicates that a variant within or very close to a gene influences its expression. Genes with *cis-eQTLs* are high priority candidates, as it provides a potential causal pathway between the gene variant and the phenotype of interest (i.e., the variant alters gene expression, and the expression of that gene alters the phenotype). Therefore, if a gene within a QTL interval is *cis-regulated*, we categorize it as a high priority candidate. For each QTL, we identified which, if any, genes within the QTL interval also had a *cis-eQTL*, and in which tissues an eQTL was seen (using transcriptome data from GeneNetwork.org). Using this same data, we also identified correlations between expression of each of these genes and the phenotype of interest.

### 2.7. “Gene Friends”, or Co-Expression Analysis

Genes with a *cis-eQTL* in at least one tissue were further considered for co-expression analysis. The top 10,000 correlations were generated in the tissue with the highest correlation between gene expression and the phenotype of interest. Gene-gene correlations with Sample  $p(r) < 0.05$  were taken into WebGestalt to perform an over-representation analysis [42–45]. This results in the identification of significantly enriched annotations or pathways in the genes which co-express with our gene of interest. This can often suggest pathways or networks that the gene is involved in, even if the gene itself has not yet been annotated as part of that network.

### 2.8. Gene Variant Analysis

Deep, linked-read sequencing of the 152 members of the BXD family was carried out using Chromium 10X sequencing (<https://www.10xgenomics.com/products/linked-reads>, accessed on 2 February 2022), resulting in 5,390,695 SNPs and 733,236 indels, which are high confidence and segregate in the population (i.e., have a minor allele frequency greater than 0.2). These 6 million variants are potential causes of QTLs detected in the BXD family.

To identify potential effects of these variants, we used the Variant Effect Predictor (VEP) website (<http://ensembl.org/Tools/VEP>, accessed on 2 February 2022 [46]). All variants within our QTL intervals were extracted from the variant VCF file and uploaded to the VEP. Potentially deleterious variants or variants which impact protein function were identified using the “Consequence”, “IMPACT”, “SIFT” [47,48] and “BLOSUM62” [49] annotations.

### 2.9. PheWAS

Phenome-wide association studies (PheWAS) utilize a genomic region of interest to find associations between that region and phenotypes measured in GWAS datasets. We used human PheWAS data for all the candidate genes in our QTLs to detect genes with relevant human phenotype associations (i.e., behavioural and neurological phenotypes). A relevant association implies confidence in a candidate gene and suggests cross-species translatability of the finding. We used online PheWAS tools, GWASatlas (<https://atlas.ctglab.nl/PheWAS>, accessed on 2 February 2022, [50]) and PheWeb (<http://pheweb.sph.umich.edu/>, accessed on 2 February 2022) for this study.

## 3. Results

### 3.1. Identification of QTLs

We first sought to identify novel genetic loci linked to the phenotypes from Philip et al., 2010 [39] that were not found in the original study. Comparing QTL mapping using Haley–Knot (H-K; as used previously) [51] and GEMMA, there are 426 traits which had a maximum LRS < 17 with H-K (i.e., non-significant), that now have a maximum  $-\log(p) > 4$ . These new QTL are therefore of interest (Table 1). To confirm these, we performed

linear mixed model (LMM) QTL mapping in R/qtl2, with permutations. This produced 61 traits which are significant compared to the empirical significance threshold generated by permutations (Supplementary Table S3).

**Table 1.** Summary of novel QTL, not found at the significant or suggestive level in the original paper by Philip et al. [39]. The position of the QTL, a summary of the phenotypes within that QTL, and relevant phenotypes found in other studies are shown. Details of all identified QTL are in Supplementary Table S5.

Chromosome	QTL Confidence Interval (Mb)	Summary of Phenotype	Relevant Behaviour Phenotype	PMID of Relevant Phenotype
Chr1	37.671–78.94	Locomotion	Loss of righting induced by ethanol	8974320
Chr1	37.671–78.94	Locomotion	Vertical clinging	10086232
Chr1	68.798–80.329	Cocaine and locomotion	Loss of righting induced by ethanol	16803863
Chr1	91.214–99.884	Vertical activity	Loss of righting induced by ethanol	16803863
Chr3	51.723–56.473	Vertical activity		
Chr7	97.466–104.149			
Chr12	82.859–96.105	BXD_11407		
Chr14	109.994–114.751	BXD_12023		
Chr15	71.035–77.148	Motor coordination, anxiety	Abnormal fear/anxiety-related behaviour	10556431

Two methods were used to identify QTLs of interest. First, the group of 61 traits that were significant by permutations were analysed. The second method was to take advantage of independent traits which share QTL at the same location with suggestive  $p$ -values ( $p < 0.63$ ). Traits were referred to as independent if they were carried out in separate groups of animals (e.g., males and females) or if the traits were measured at independent timepoints (e.g., at 10 min after treatment and 60 min after treatment). We identified 25 QTL for 267 traits (Supplementary Table S4).

### 3.2. Novel QTL

For each of the QTL identified above, we determined if they were reported in Philip et al.'s original study [39], or if related phenotypes have been reported in the MGI database [52].

Several locomotion traits related the QTL map to Chr1:37.671–78.94 Mb (Figure 1) that were not detected in the Philip et al. study. Previously detected relevant phenotypes associated with this region include the loss of righting reflex induced by ethanol [53] and vertical clinging [54].

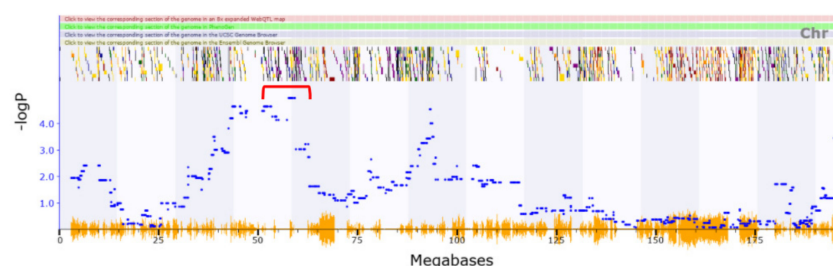


**Figure 1.** Phenotypic traits associated with locomotion map to a QTL region on chromosome 1. The peak in this region occurs between Chr1:37.67–78.94 as indicated by the red bracketed bar above. The multi-coloured lines corresponding to the dots are genes contained in this region. Blue dots correspond to areas with specific  $-\log P$  scores relating to the phenotype.



We report a novel QTL on Chromosome3 (51.723–56.473 Mb) for vertical clinging activity, and on Chromosome4 (105.245–114.11 Mb) for locomotion in response to cocaine. Previous studies show a QTL for anxiety in this region of Chromosome4 [55]. We also report novel QTLs on Chromosome5 for handling induced convulsions as an ethanol response (4.468–5.172 Mb) as well as locomotion in response to cocaine (99.801–101.331 Mb). Finally, there was a novel QTL for locomotion in response to cocaine on Chromosome11 (46.361–50.383 Mb) (Supplementary Table S4).

### 3.3. Candidate Causal Genes within Novel QTL

We concentrated on a subset of six novel QTL that contained less than 100 genes. These QTLs are more amenable to finding plausible candidate genes using bioinformatic methods. After reducing the likelihood of finding false positives, these large QTLs are more likely to be due to two or more variants in different genes both contributing to the phenotype. The advantage of families of isogenic strains of mice, such as the BXD, is that more strains could be phenotyped, reducing the size of these QTL regions and allowing for greater precision. We leave these large QTLs to future studies. The smaller QTL regions investigated here were: Chr3:51.723–56.473 Mb, Chromosome5:4.468–5.172 Mb, Chr5:99.801–101.331 Mb, Chr9:45.671–48.081 Mb, Chr11:62.923–65.082 Mb and Chromosome14:109.994–114.751 Mb (Supplementary Table S4)

We used several tools to narrow down potential candidate genes within these QTLs. Variants can change phenotype in two main ways: they can either change gene expression or can change protein function. To look for variants altering gene expression, we first looked for genes within our QTL regions with local or cis-eQTL. Cis-eQTL demonstrate that there are variants in or close to a gene that cause changes in that gene's expression. This is useful, since it clearly shows that a variant in the eQTL region has a regulatory effect. Therefore, genes with a cis-eQTL are interesting candidate genes.

The next step is to investigate whether the expression of these genes correlates with the phenotype(s) of interest. This would suggest a chain of causality: a variant within a gene causes a change in its expression, and the expression of that gene correlates with expression of a phenotypic trait of interest. To do this, we created a correlation matrix between all genes within a QTL with a cis-eQTL in any brain tissue as well as the phenotypes that contributed to the QTL (Supplementary Table S6). Any gene with a cis-eQTL and a significantly correlated expression was considered a good candidate. If the gene only had a cis-eQTL and correlation in a single brain region, then it suggested that this brain region might also be of interest for the phenotype (adding another link to this chain).

The QTL region for vertical activity (Chromosome3 51.723–56.473 Mb) has 60 genes among which six genes have cis-eQTLs (Figure 2) (Supplementary Table S6). No relevant functional annotations (Gene Ontology) have been reported. *Dcl1* (location of cis-eQTL: Chromosome3 55.52 Mb) variants were previously reported to be associated across Schizophrenia and Attention Deficit Hyperactivity Disorder [56]. The same gene has been described as a candidate gene for inflammatory nociception [57]. *Trpc4* (location of cis-eQTL: Chromosome3 54.266176 Mb) may be involved in the regulation of anxiety-related behaviours [58].

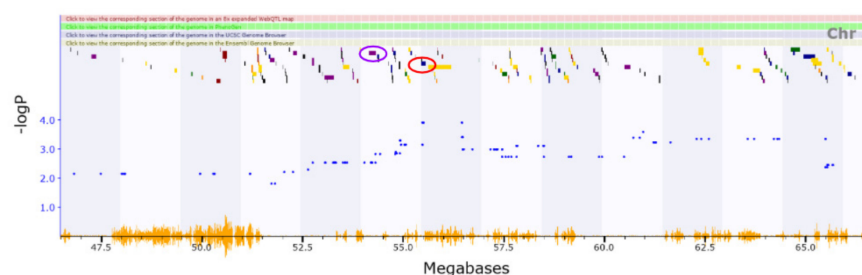


**Figure 2.** (55.52 Mb) shown in the red circle, and *Trpc4* shown in the purple circle (54.27 Mb), which both have cis-eQTLs in this region. Although these genes have not been annotated for this specific phenotype, they are implicated in previous studies with associated behaviors.

The QTL region for handling induced convulsions (ethanol response; Chromosome5 4.468–5.172 Mb) house two genes (*Fzd1* and *Cdk14*) with cis-eQTLs among the three present in this region. *Fzd1* (location of cis-eQTL: Chromosome5 4.753 Mb) receptor regulates adult hippocampal neurogenesis [59]. The QTL corresponding with locomotion in response to cocaine (Chromosome5 99.801–101.331 Mb) has ten genes with cis-eQTLs (Figure 3). QTL analysis of *Enoph1* (location of cis-eQTL: Chromosome5 100.062 Mb) in mice indicates that it plays a role in stress reactivity [60]. Variants of *Coq2* (location of cis-eQTL: Chromosome5 100.654 Mb) contribute to neurodegenerative disorders such as Parkinson’s disease [61].

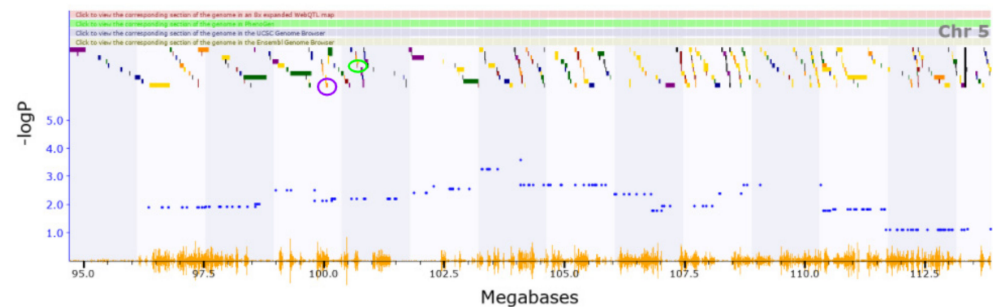


**Figure 3.** A QTL corresponding with locomotion in response to cocaine has ten genes with cis-eQTLs for Trait ID BXD\_11487. A QTL containing *Enoph1* shown in the purple circle (100.062 Mb) has been implicated in previous research for its role in stress reactivity. *Coq2* shown in the green circle (100.654 Mb) has been investigated for its contribution to neurodegenerative disorders. Although these two genes are great candidates for genes of interest, these aren’t the only applicable. Other relevant genes in this section have not been reported yet by other studies.

Relevant annotations for other genes with cis-eQTLs have not been reported yet by other studies. The QTL corresponding with mechanical nociception (Chromosome9 45.671–48.081 Mb) includes five genes with cis-eQTLs. *Sik3* (location of cis-eQTL: Chromosome9 46.222 Mb) is involved in regulating NREM sleep behaviour in mice [62]. *Cadm1* (location of cis-eQTL: Chromosome9 47.550 Mb) knockout mice show increased anxiety, impaired social and emotional behaviours, and disrupted motor coordination (Figure 4) [63].

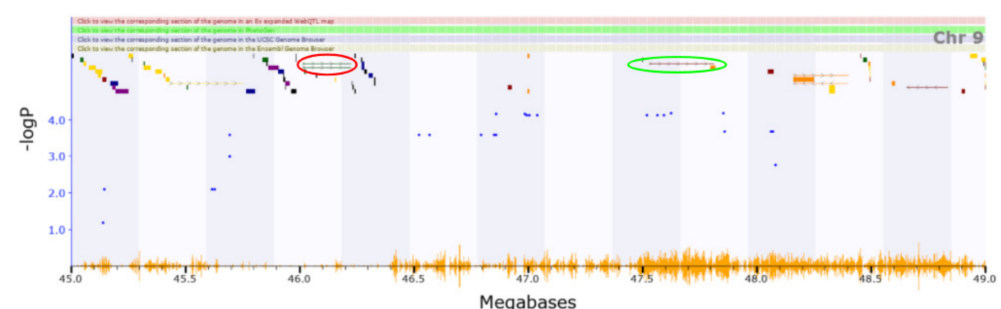


**Figure 4.** Shown in the red circle (46.22 Mb) is involved in regulating sleep behaviors. *Cadm1* shown in the green circle (47.55 Mb) is associated with increased anxiety, impaired social and emotional behaviors, and disrupted motor coordination in knockout mice.

An analysis of the locomotion in response to cocaine QTL (Chromosome11 62.923–65.082 Mb) revealed five genes with cis-eQTLs. *Arhgap44* (location of cis-eQTL: Chromosome11 65.005456 Mb) has phenotype associations related to abnormal motor learning, abnormal response to novel objects, increased grooming behaviour, and hypoactivity (Figure 5) [64]. The brain regions with highest correlation have been added to the Supplementary Information (Supplementary Table S6). The QTL corresponding to locomotion in the centre (Chromosome14 109.994–114.751 Mb) has a single gene with a cis-eQTL, *Slitrk6* (location of cis-eQTL:

Chromosome14 109.231826 Mb, in Figure 6). Knockout of this gene has been associated with impaired locomotory behaviour and altered responses to a novel environment, making this gene a strong candidate [65].

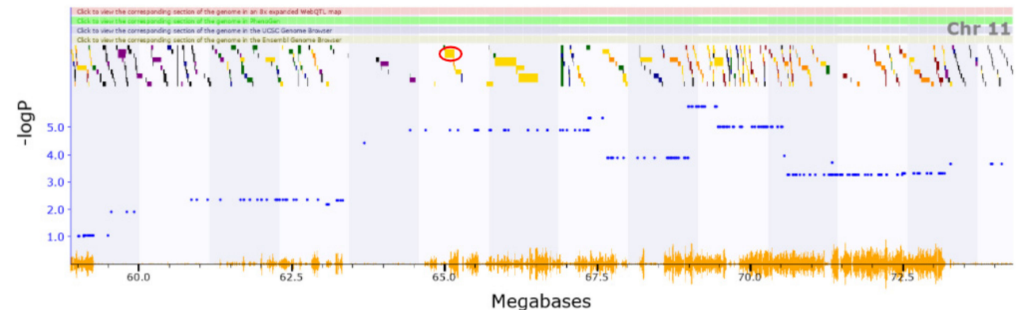


**Figure 5.** A QTL for motor activity in response to cocaine revealed five genes with cis-eQTLs. *Arhgap44* shown in the red circle (65.01 Mb) associates with abnormal motor learning, abnormal response to novel objects, increased grooming behavior, and hypoactivity.

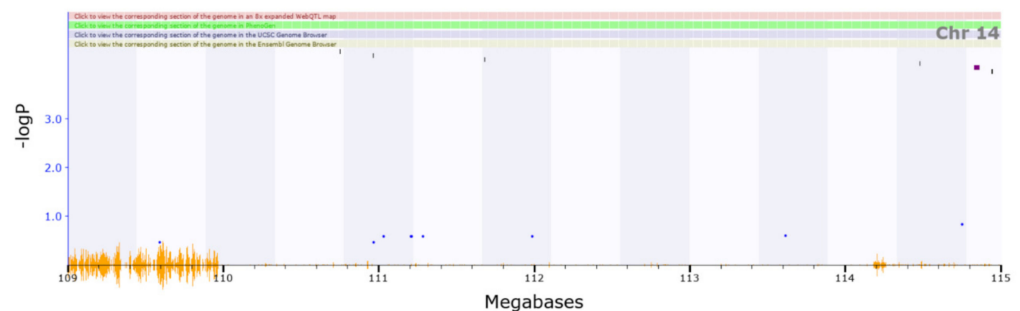


**Figure 6.** There is a single gene with a cis-eQTL corresponding to the QTL region on chromosome 14. *Slitrk6* (109.23 Mb), loss of this gene in mice has been associated with impaired locomotory behavior as well as altered responses to novel environmental cues.

### 3.4. Co-Expression Networks or “Gene-Friends”

Genes that are co-expressed are often part of the same pathways or networks which contribute to similar phenotypes. These so-called ‘gene-friends’ [66,67] can provide insights into the function of an unannotated gene as function can be implied from the known functions of the genes it co-expresses with. As new datasets are being generated for the BXD consistently (now including methylation, proteomic and metabolic datasets), new associations can be found.

For each of the genes within our phenotype QTLs that also has a cis-eQTL in at least one dataset on GeneNetwork.org, we performed a correlation analysis with all other probes or genes within that dataset. We then performed an enrichment analysis using WebGestalt using all the probes or genes that correlated with our gene of interest (i.e., the gene with a cis-eQTL), and investigated if any of the enriched annotations or pathways were relevant to the phenotype.

Highly relevant enriched phenotypes were found in genes co-expressing with *9430012M22Rik* (location of cis-eQTL: Chromosome3 55.291 Mb). This gene is present in a QTL for vertical activity (BXD\_12023). Genes that correlate with expression of *9430012M22Rik* in the neocortex are enriched for involvement in abnormal locomotor behaviour ( $FDR = 1.2056 \times 10^{-9}$ ) and abnormal voluntary movement ( $FDR = 7.1848 \times 10^{-10}$ ). Other results for this co-expression network that may be relevant include abnormal synaptic transmission and abnormal nervous system physiology (Supplementary Table S7). The genes that correlate with expression of *BC033915* (location of cis-eQTL: Chr9 45.671–48.081 Mb) in the hippocampus are enriched for abnormal motor capabilities/coordination/movement ( $FDR = 2.3483 \times 10^{-11}$ ). Other relevant results



include abnormal brain morphology and abnormal nervous system physiology. Similarly, genes in the *Slitrk6* co-expression network (location of cis-eQTL: Chromosome14 109.231 Mb) in the striatum are involved in abnormal locomotor behaviour ( $FDR = 6.978 \times 10^{-12}$ ) and abnormal voluntary movement ( $FDR = 2.9352 \times 10^{-11}$ ). This makes sense, since this Chromosome14 QTL is for locomotion.

Other genes with cis-eQTLs had significant enrichments that include abnormal brain morphology, abnormal body composition and abnormal nervous system physiology (Supplementary Table S7).

### 3.5. Gene Variant Analysis

The second method by which a variant can alter a phenotype is changing the protein structure or function. To examine this, we took advantage of the deep sequencing available for all BXD strains. We identified over 6 million common SNPs and small INDELs which segregate within the BXD family (i.e., occur in greater than >20% of the population). For each of the 6 QTL identified above, we looked for variants that were predicted to alter protein structure or splicing, or predicted to be deleterious by SIFT or BLOSUM, using the variant effect predictor (VEP).

The QTL located at Chr3:53.667–54.942Mb for vertical activity contains predicted deleterious variants in 10 genes (Table 2): two missense variants in *Ccdc169*; one missense variant in *Ccna1*; one in-frame insertion in *Dclk1*; two frameshift variants, a stop loss, and nine missense variants in *Frem2*; a frameshift variant and six missense variants in *Mab21l1*; a frameshift variant, a missense variant, eight frameshift variants, two in-frame deletions, 18 missense variants, and three stop losses in *Nbea*; four in-frame deletions, an in-frame insertion, six missense variants, and a start loss in *Postn*; a frameshift variant, eight missense variants, a stop gain, and a stop loss in *Spg20*; and a missense variant in *Trpc4*.

**Table 2.** QTL located at Chr3:53.667–54.942Mb for vertical activity contains predicted deleterious variants in 10 genes.

Number of Variants	Type of Variant	Gene
2	Missense	<i>Ccdc169</i>
1	Missense	<i>Ccna1</i>
1	In-frame insertion	<i>Dclk1</i>
2	Frameshift	<i>Frem2</i>
1	Stop loss	<i>Frem2</i>
9	Missense	<i>Frem2</i>
1	Frameshift	<i>Mab21l1</i>
6	Missense	<i>Mab21l1</i>
9	Frameshift	<i>Nbea</i>
2	In-frame deletions	<i>Nbea</i>
19	Missense	<i>Nbea</i>
3	Stop loss	<i>Nbea</i>
4	In-frame deletions	<i>Postn</i>
1	In-frame insertions	<i>Postn</i>
6	Missense	<i>Postn</i>
1	Start loss	<i>Postn</i>
1	Frameshift	<i>Spg20</i>
8	Missense	<i>Spg20</i>
1	Stop gain	<i>Spg20</i>
1	Stop loss	<i>Spg20</i>
1	Missense	<i>Trpc4</i>

The Chr5:4.468–5.172Mb QTL for handling-induced convulsion in response to ethanol contains two missense variants in *Fzd1*, and four missense variants in *Cdk14*. The Chr5:100.164–100.895Mb QTL for cocaine related phenotypes, contains predicted deleterious variants in 8 genes (Table 3): three frameshift variants and three missense variants in *Cops4*; a missense variant and a stop-gain in *Enoph1*; a frameshift variant and five missense variants in *Hnrnpd*; three missense

variants and a splice donor variant in *Hnrnpdl*; two frameshift variants, an in-frame insertion, 13 missense variants, and a splice donor variant in *Hpse*; three missense variants in *LIN54*; a frameshift variant, one in-frame deletions, and a splice donor variant in *Sec31a*; and a missense variant and a splice donor variant in *Tmem150c*.

**Table 3.** The Chr5:100.164–100.895Mb QTL for cocaine related phenotypes contains predicted deleterious variants in 8 genes.

Number of Variants	Type of Variant	Gene
3	Frameshift	<i>Cops4</i>
3	Missense	<i>Cops4</i>
1	Missense	<i>Enoph1</i>
1	Stop gain	<i>Enoph1</i>
1	Frameshift	<i>Hnrnpd</i>
5	Missense	<i>Hnrnpd</i>
3	Missense	<i>Hnrnpd</i>
1	Splice donor	<i>Hnrnpd</i>
2	Frameshift	<i>Hpse</i>
1	In-frame insertion	<i>Hpse</i>
13	Missense	<i>Hpse</i>
1	Splice donor	<i>Hpse</i>
3	Missense	<i>Lin54</i>
1	Frameshift	<i>Sec31a</i>
1	In-frame deletion	<i>Sec31a</i>
1	Splice donor	<i>Sec31a</i>
1	Missense	<i>Tmem150c</i>
1	Splice donor	<i>Tmem150c</i>

The QTL located in chromosome 9 at 45.671–48.081Mb for mechanical nociception contains predicted deleterious variants in three genes (Table 4): A frameshift variant, two missense variants and a stop loss in *4931429L15Ri*; two frameshift variants and five missense variants in *Cadm1*; and an in-frame deletion, three missense variants, and a stop loss in *Cep164*. The Chr11:62.923–65.082Mb QTL for nociception contains four frameshift variants, an in-frame deletion, and thirteen missense variants in *Myocd*. The Chr14:109.994–114.751 Mb QTL for locomotion contains a stop loss, three frameshift variants, and 9 missense variants in *Slitrk6*.

**Table 4.** The QTL located in chromosome 9 at 45.671–48.081Mb for mechanical nociception contains predicted deleterious variants in 3 genes.

Number of Variants	Type of Variant	Gene
1	Frameshift	<i>4931429L15Ri</i>
2	Missense	<i>4931429L15Ri</i>
1	Stop gain	<i>4931429L15Ri</i>
2	Frameshift	<i>Cadm1</i>
5	Missense	<i>Cadm1</i>
1	In-frame deletion	<i>Cep164</i>
3	Missense	<i>Cep164</i>
1	Stop loss	<i>Cep164</i>

### 3.6. PheWAS Analysis of the Genes within QTLs

Another method to identify candidate genes is to leverage data generated in another population or species. Phenome-wide association studies (PheWAS) take a gene or variant of interest and find all reported associations in GWAS datasets. A number of these GWAS tools exist, using either different methods, or different human cohorts (<https://atlas.ctglab.nl/PheWAS>, <http://pheweb.sph.umich.edu/>, accessed on 2 February 2022).

Mouse QTL mapping has high power but low precision (i.e., we can detect a QTL, but do not know which of tens or hundreds of genes is causal), whereas human GWAS has low power but high precision (tens or hundreds of thousands of individuals are needed, but

candidate regions are often smaller). By combining the power of mouse QTL mapping and the precision of human PheWAS, we can do more than both individually. Candidate genes might show up in our analysis here that did not show up in our above analysis for several reasons, the most common being that gene expression was not measured in the relevant cell type or timepoint.

The QTL for vertical activity (Chromosome3 51.723–56.473 Mb) includes several genes with relevant psychiatric, neurological, and cognitive PheWAS hits. *Maml3* is associated with alcohol dependence [68] and depression (Figure 7 and Table 5) [69]. *Cog6* has significant associations with depressive symptoms [70] and worrier/anxious feelings [50]. *Nbea* is associated with nervous feelings [50] and alcohol dependence [68].

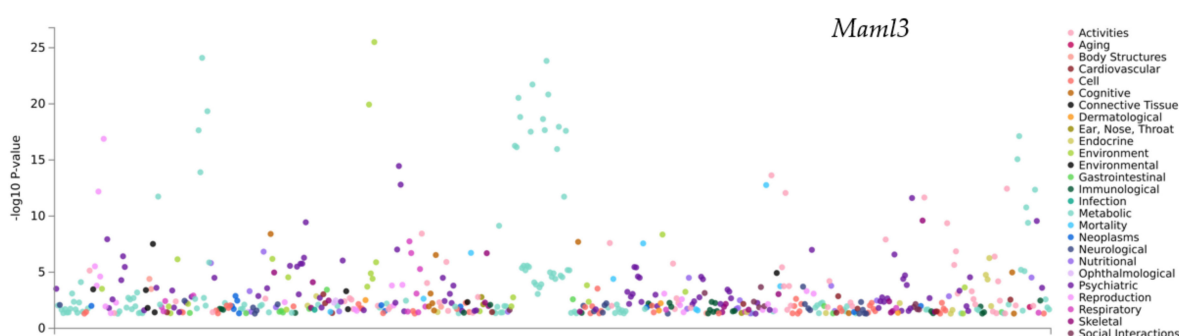


**Figure 7.** QTLs linked with murine phenotypes gain precision with the use of relevant PheWAS hits in a GWAS atlas. An example for this is for vertical activity (Chr 3 51.723–56.473 Mb) includes a number of genes with relevant psychiatric, neurological and cognitive PheWAS hits. *Maml3* is associated with alcohol dependence and depression.

**Table 5.** QTLs linked with murine phenotypes gain precision with the use of relevant PheWAS hits in a GWAS atlas. An example for this is for vertical activity (Chr 3 51.723–56.473 Mb) includes a number of genes with relevant psychiatric, neurological and cognitive PheWAS hits. *Maml3* is associated with alcohol dependence and depression.

atlas ID	PMID	Year	Domain	Trait	p-Value	N
4314	30643251	2019	Psychiatric	Ever smoked regularly	$3.47 \times 10^{-15}$	262990
3654	31427789	2019	Psychiatric	Smoking status: Never	$2.45 \times 10^{-12}$	384964
4327	30643256	2019	Psychiatric	Well-being spectrum	$2.73 \times 10^{-10}$	2311184
4322	30643256	2019	Psychiatric	Depressive symptoms (univariate)	$3.58 \times 10^{-10}$	1067913
4313	30643251	2019	Psychiatric	Age of initiation of regular smoking	$1.16 \times 10^{-8}$	632802
3425	31427789	2019	Psychiatric	Ever smoked	$9.55 \times 10^{-8}$	385013
3236	31427789	2019	Psychiatric	Past tobacco smoking	$1.02 \times 10^{-7}$	355594
4274	30846698	2019	Psychiatric	Short sleep	$2.64 \times 10^{-7}$	411934
3261	31427789	2019	Psychiatric	Alcohol intake frequency	$3.80 \times 10^{-7}$	386082
4326	30643256	2019	Psychiatric	Depressive symptoms (MA GWAMA)	$5.12 \times 10^{-7}$	1067913
56	27089181	2016	Psychiatric	Depressive symptoms	$1.72 \times 10^{-6}$	161460
3796	29942085	2018	Psychiatric	Depressive symptoms	$1.75 \times 10^{-6}$	381455
3235	31427789	2019	Psychiatric	Current tobacco smoking	$2.71 \times 10^{-6}$	386150
4293	30718901	2019	Psychiatric	Depression	$3.19 \times 10^{-6}$	500199
3268	31427789	2019	Psychiatric	Alcohol intake versus 10 years previously	$3.41 \times 10^{-6}$	357907
4171	29970889	2018	Psychiatric	Loneliness	$3.44 \times 10^{-6}$	445024
4170	29970889	2018	Psychiatric	Loneliness (MTAG)	$3.72 \times 10^{-6}$	487647

All the three genes present in the Chr5 4.468–5.172 Mb QTL (handling-induced convulsions, ethanol response) show significant PheWAS hits for psychiatric traits. *Fzd1* (location of cis-eQTL: Chromosome5 4.753 Mb) is significantly associated with major depressive disorder [71]. In the QTL residing in Chromosome5, the peak 99.801–101.331 Mb region contains the genes *Hnrnpd* and *Lin54*, which show the highest number of relevant pheWAS hits. *Lin54* is associated with conditions such as loneliness, anxiety, tension, and sleep related phenotypes (Figure 8 and Table 6) [50,72,73].

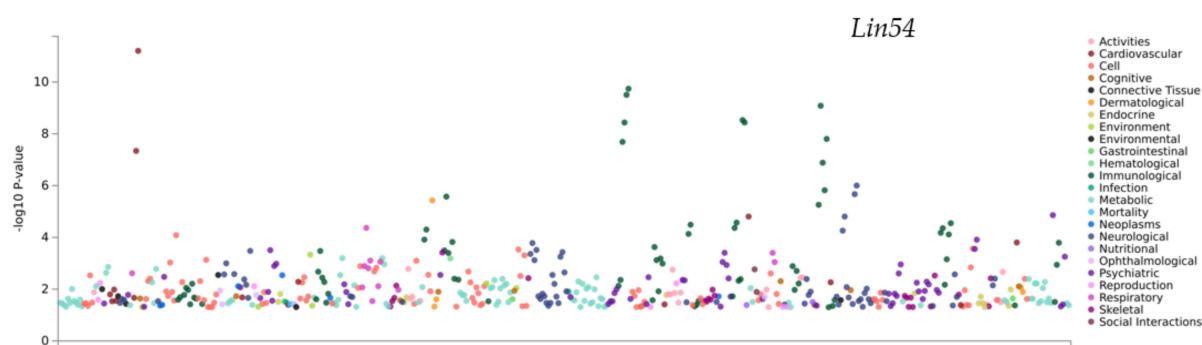


**Figure 8.** Combining PheWAS hits in GWAS atlases with BXD data allow for more robust screening of variants that affect phenotypes. The QTL at Chr 5 peaks at 99.801–101.331 Mb and contains the genes *Hnrnpd* and *Lin54*, which show the highest number of relevant pheWAS hits. *Lin54* is listed by trait above and has been previously associated with psychiatric phenotypes.

**Table 6.** Combining PheWAS hits in GWAS atlases with BXD data allow for more robust screening of variants that affect phenotypes. The QTL at Chr 5 peaks at 99.801–101.331 Mb and contains the genes *Hnrnpd* and *Lin54*, which show the highest number of relevant pheWAS hits. *Lin54* is listed by trait above and has been previously associated with psychiatric phenotypes.

atlas ID	PMID	Year	Domain	Trait	p-Value	N
4327	30643256	2019	Psychiatric	Well-being spectrum	$1.40 \times 10^{-5}$	2311184
3998	29500382	2018	Psychiatric	Tense	$1.23 \times 10^{-5}$	263635
3291	31427789	2019	Psychiatric	Tense	$2.80 \times 10^{-4}$	374129
4293	30718901	2019	Psychiatric	Depression	$3.12 \times 10^{-4}$	500199
4325	30643256	2019	Psychiatric	Neuroticism (MA GWAMA)	$3.94 \times 10^{-4}$	523783
3798	29942085	2018	Psychiatric	Worry subcluster	$5.57 \times 10^{-4}$	348219
4087	29255261	2018	Psychiatric	Neuroticism	$8.90 \times 10^{-4}$	329821
4322	30643256	2019	Psychiatric	Depressive symptoms (univariate)	$1.05 \times 10^{-3}$	1067913
3301	31427789	2019	Psychiatric	Seen doctor (GP) for nerves, anxiety, tension or depression	$1.11 \times 10^{-3}$	383771
4321	30643256	2019	Psychiatric	Neuroticism (univariate)	$1.12 \times 10^{-3}$	523783
4326	30643256	2019	Psychiatric	Depressive symptoms (MA GWAMA)	$1.27 \times 10^{-3}$	1067913
3302	31427789	2019	Psychiatric	Seen a psychiatrist for nerves, anxiety, tension or depression	$2.48 \times 10^{-3}$	384700
3745	31427789	2019	Psychiatric	Happiness and subjective well-being—General happiness	$2.83 \times 10^{-3}$	126132
4011	29662059	2018	Psychiatric	Broad depression	$3.34 \times 10^{-3}$	322580
4013	29662059	2018	Psychiatric	Major depressive disorder (ICD-coded)	$3.46 \times 10^{-3}$	217584
4269	30867560	2019	Psychiatric	Neuroticism general factor	$3.84 \times 10^{-3}$	270059
3230	31427789	2019	Psychiatric	Morning/evening person (chronotype)	$4.42 \times 10^{-3}$	345148

*Cadm1* (Location of *cis*-eQTL: Chromosome9 47.550 Mb) gene was found significantly associated with schizophrenia and other psychiatric disorders [71,74]. Among the genes with *cis*-eQTLs in Chromosome11, *Elac2* (location of *cis*-eQTL: Chr11 64.988 Mb) and *Arghap44* have most significant phenotype associations with schizophrenia/bipolar disorder [74,75]. The QTL for locomotion in the centre (Chr14 109.994–114.751 Mb) shows one gene with a PheWAS hit. *Slitrk6* is significantly associated with Parkinson's disease [76] and bipolar disorder [75], as well as has significant associations with various psychiatric traits

including anxiety [50], nervous feelings [50] and alcohol dependence [68] (Supplementary Table S8).

#### 4. Discussion

Here, we have demonstrated that old data in populations of isogenic strains can be reanalysed to identify novel genetic associations containing novel candidate genes. Of particular interest is *Slitrk6* on Chr14. *Slitrk6* (SLIT and NTRK Like Family Member 6) is a protein coding gene. Our analysis strongly shows that abnormality in *Slitrk6* is implicated in disrupted locomotor behaviour. The presence of cis-eQTL implies that a variant in this gene is affecting its expression and the gene is under its own regulation. Being part of a network in the striatum, which is significantly involved in abnormal locomotory behaviour and abnormal voluntary movement, increases the plausibility. This gene has evidence of both altered gene expression and protein structure/function, and human PheWAS analysis shows that this gene is involved in various neuropsychiatric and neurological phenotypes. The *Slitrk* family have been previously mentioned as prominent candidate genes involved in neuropsychiatric disorders [77]. The members of the *Slitrk* family have been shown to be widely expressed in the central nervous system, with partially overlapping yet differential patterns of expression [78]. It is worth noting that this gene along with the other candidates have not been reported in the original study.

Another prominent finding is *Cadm1* (Cell adhesion molecule 1), which is a member of the immunoglobulin superfamily and present on Chromosome9. Our analysis shows the presence of a cis-eQTL for this gene, and variants in the human gene are associated with schizophrenia. *Cadm1* knockout mice show anxiety-like behaviour in the open-field and light-dark transition tests, as well as motor coordination and gait impairments in rotarod and footprint tests [63]. The role of CADM1 in relation to prefrontal brain activities, inhibition function, and ADHD, indicating a potential “gene–brain–behaviour” relationship was shown previously by research that evaluated the association of CADM1 genotype with ADHD, executive function, and regional brain functions [79]. Studies show a connection between ADHD and pain tolerance [80], and adults with ADHD are comparatively more sensitive to pain. In such cases, dopamine agonists such as methylphenidate (MP) may exert antinociceptive properties [81] and normalize pain perception. Adults and children with ADHD exhibit motor regulation problems which are in turn associated with pain levels [82].

We discovered a novel QTL that regulates and handles induced convulsions after ethanol treatment (BXD\_11635) on Chr5:4.468–5.172. Only three genes are within the confidence interval for this QTL, two of which, *Fzd1* and *Cdk14*, have cis-eQTL and predicted deleterious variants. Interestingly, *Cdk14* is regulated by the anticonvulsant drug valproic acid [83–85] and is up-regulated in malaria patients who experience febrile convulsions [41,51,86].

#### 5. Conclusions

In this analysis, using GeneNetwork.org (<http://www.genenetwork.org/>, accessed on 2 February 2022), we have demonstrated the plausibility of using new tools to re-examine older data to investigate candidate genes relevant to addiction research. We used families of isogenic strains of mice to not only go back and discover new drug-related phenotype–genotype associations that were not previously found, but also find highly plausible candidate genes within these novel QTL. Of these genes, many were found to have implications for phenotypes of interest in addiction research, as well as translatability across mouse and human datasets. This sort of investigation is key in the study of addiction-related illnesses, since these diseases are complex and polygenic in nature, and also possess explicit environmental components.

**Supplementary Materials:** The following supporting information can be downloaded at: <https://www.mdpi.com/article/10.3390/genes13040614/s1>, Table S1: Phenotype data and reanalysis with new tools and genotypes; Table S2: Significant traits with QTL regions; Table S3: Significant traits (H-K vs. GEMMA and R/qt12); Table S4: QTLs and respective summaries; Table S5: Comparison of



QTLs found in this study with Philip et al. and other studies; Table S6: Genes and cis-eQTLs; Table S7: Co-expression networks or ‘gene-friends’; Table S8: PheWAS.

**Author Contributions:** Conceptualization, A.C. and D.G.A.; methodology, A.C. and P.M.W.; formal analysis, D.G.A.; investigation, A.C. and P.M.W.; resources, D.G.A.; data curation, A.C. and D.G.A.; writing—original draft preparation, A.C.; writing—review and editing, P.M.W.; visualization, P.M.W.; supervision, D.G.A.; project administration, D.G.A. All authors have read and agreed to the published version of the manuscript.

**Funding:** This project was carried out using GeneNetwork.org. GeneNetwork.org is supported by the UTHSC Center for Integrative and Translational Genomics, the UT-ORNL Governor’s Chair, NIGMS R01GM123489, NIDA P30DA044223, NIAAA U01AA016662, U01AA013499, U24AA013513, U01AA014425, and NIAAA P20DA21131.

**Institutional Review Board Statement:** Not applicable.

**Informed Consent Statement:** Not applicable.

**Data Availability Statement:** All data supporting this article can be accessed and reanalyzed using GeneNetwork.org.

**Acknowledgments:** We would like to thank the authors of Philip et al. 2010. Without their work in producing the data, and in making it freely available on GeneNetwork.org, this project would not have been possible. We thank R.W. Williams for helpful discussion on the BXD models. We thank the members of the GeneNetwork.org team for their assistance, excellent data curation, and informatics support.

**Conflicts of Interest:** The authors declare no conflict of interest.

## References

1. Wilkinson, M.D.; Dumontier, M.; Aalbersberg, I.J.; Appleton, G.; Axton, M.; Baak, A.; Blomberg, N.; Boiten, J.W.; da Silva Santos, L.B.; Bourne, P.E.; et al. The FAIR Guiding Principles for scientific data management and stewardship. *Sci. Data* **2016**, *3*, 160018. [\[CrossRef\]](#)
2. Ashbrook, D.G.; Arends, D.; Prins, P.; Mulligan, M.K.; Roy, S.; Williams, E.G.; Lutz, C.M.; Valenzuela, A.; Bohl, C.J.; Ingels, J.F.; et al. A platform for experimental precision medicine: The extended BXD mouse family. *Cell Syst.* **2021**, *12*, 235–247.e9. [\[CrossRef\]](#)
3. Castle, W.E. Variation in the hooded pattern of rats, and a new allele of hooded. *Genetics* **1951**, *36*, 254–266. [\[CrossRef\]](#)
4. Belknap, J.K.; Crabbe, J.C.; Plomin, R.; McClearn, G.E.; Sampson, K.E.; O’Toole, L.A.; Gora-Maslak, G. Single-locus control of saccharin intake in BXD/Ty recombinant inbred (RI) mice: Some methodological implications for RI strain analysis. *Behav. Genet.* **1992**, *22*, 81–100. [\[CrossRef\]](#)
5. Belknap, J.K.; Metten, P.; Helms, M.L.; O’Toole, L.A.; Angeli-Gade, S.; Crabbe, J.C.; Phillips, T.J. Quantitative trait loci (QTL) applications to substances of abuse: Physical dependence studies with nitrous oxide and ethanol in BXD mice. *Behav. Genet.* **1993**, *23*, 213–222. [\[CrossRef\]](#)
6. Dickson, P.E.; Miller, M.M.; Calton, M.A.; Bubier, J.A.; Cook, M.N.; Goldowitz, D.; Chesler, E.J.; Mittleman, G. Systems genetics of intravenous cocaine self-administration in the BXD recombinant inbred mouse panel. *Psychopharmacology* **2016**, *233*, 701–714. [\[CrossRef\]](#)
7. Grisel, J.E.; Belknap, J.K.; O’Toole, L.A.; Helms, M.L.; Wenger, C.D.; Crabbe, J.C. Quantitative trait loci affecting methamphetamine responses in BXD recombinant inbred mouse strains. *J. Neurosci.* **1997**, *17*, 745–754. [\[CrossRef\]](#)
8. Palmer, A.A.; Lessov-Schlaggar, C.N.; Ponder, C.A.; McKinnon, C.S.; Phillips, T.J. Sensitivity to the locomotor-stimulant effects of ethanol and allopregnanolone: A quantitative trait locus study of common genetic influence. *Genes Brain Behav.* **2006**, *5*, 506–517. [\[CrossRef\]](#)
9. Phillips, T.J.; Belknap, J.K.; Buck, K.J.; Cunningham, C.L. Genes on mouse chromosomes 2 and 9 determine variation in ethanol consumption. *Mamm. Genome* **1998**, *9*, 936–941.
10. Rodriguez, L.A.; Plomin, R.; Blizard, D.A.; Jones, B.C.; McClearn, G.E. Alcohol acceptance, preference, and sensitivity in mice. I. Quantitative genetic analysis using BXD recombinant inbred strains. *Alcohol. Clin. Exp. Res.* **1994**, *18*, 1416–1422. [\[CrossRef\]](#)
11. Boon, A.C.M.; Williams, R.W.; Sinasac, D.S.; Webby, R.J. A novel genetic locus linked to pro-inflammatory cytokines after virulent H5N1 virus infection in mice. *BMC Genom.* **2014**, *15*, 1017. [\[CrossRef\]](#)
12. Grizzle, W.E.; Mountz, J.D.; Yang, P.-A.; Xu, X.; Sun, S.; Van Zant, G.E.; Williams, R.W.; Hsu, H.C.; Zhang, H.G. BXD recombinant inbred mice represent a novel T cell-mediated immune response tumor model. *Int. J. Cancer* **2002**, *101*, 270–279. [\[CrossRef\]](#)
13. Hayes, K.S.; Hager, R.; Grecis, R.K. Sex-dependent genetic effects on immune responses to a parasitic nematode. *BMC Genom.* **2014**, *15*, 193. [\[CrossRef\]](#)
14. Miyairi, I.; Ziebarth, J.; Laxton, J.D.; Wang, X.; van Rooijen, N.; Williams, R.W.; Lu, L.; Byrne, G.I.; Cui, Y. Host genetics and Chlamydia disease: Prediction and validation of disease severity mechanisms. *PLoS ONE* **2012**, *7*, e33781. [\[CrossRef\]](#)

15. Wang, J.; Yoon, T.W.; Read, R.; Yi, A.-K.; Williams, R.W.; Fitzpatrick, E.A. Genetic variability of T cell responses in Hypersensitivity Pneumonitis identified using the BXD genetic reference panel. *Am. J. Physiol. Lung Cell. Mol. Physiol.* **2020**, *318*, L631–L643. [\[CrossRef\]](#)
16. Ashbrook, D.G.; Sharmin, N.; Hager, R. Offspring genes indirectly influence sibling and maternal behavioral strategies over resource share. *Proc. R. Soc. B Biol. Sci.* **2017**, *284*, 20171059.
17. Ashbrook, D.G.; Roy, S.; Clifford, B.G.; Riede, T.; Scattoni, M.L.; Heck, D.H.; Lu, L.; Williams, R.W. Born to cry: A genetic dissection of infant vocalization. *Front. Behav. Neurosci.* **2018**, *12*, 250. [\[CrossRef\]](#)
18. Dickson, P.E.; Roy, T.A.; McNaughton, K.A.; Wilcox, T.D.; Kumar, P.; Chesler, E.J. Systems genetics of sensation seeking. *Genes Brain Behav.* **2019**, *18*, e12519. [\[CrossRef\]](#)
19. Graybeal, C.; Bachu, M.; Mozhui, K.; Saksida, L.M.; Bussey, T.J.; Sagalyn, E.; Williams, R.W.; Holmes, A. Strains and stressors: An analysis of touchscreen learning in genetically diverse mouse strains. *PLoS ONE* **2014**, *9*, e87745. [\[CrossRef\]](#)
20. Knoll, A.T.; Jiang, K.; Levitt, P. Quantitative trait locus mapping and analysis of heritable variation in affiliative social behavior and co-occurring traits. *Genes Brain Behav.* **2017**, *17*, e12431. [\[CrossRef\]](#)
21. Li, Z.; Mulligan, M.K.; Wang, X.; Miles, M.F.; Lu, L.; Williams, R.W. A transposon in Comt generates mRNA variants and causes widespread expression and behavioral differences among mice. *PLoS ONE* **2010**, *5*, e12181. [\[CrossRef\]](#) [\[PubMed\]](#)
22. Mulligan, M.K.; Abreo, T.; Neuner, S.M.; Parks, C.; Watkins, C.E.; Houseal, M.T.; Shapaker, T.M.; Hook, M.; Tan, H.; Wang, X. Identification of a Functional Non-coding Variant in the GABA A Receptor  $\alpha 2$  Subunit of the C57BL/6J Mouse Reference Genome: Major Implications for Neuroscience Research. *Front. Genet.* **2019**, *10*, 188. [\[CrossRef\]](#) [\[PubMed\]](#)
23. Williams, E.G.; Mouchiroud, L.; Frochaux, M.; Pandey, A.; Andreux, P.A.; Deplancke, B.; Auwerx, J. An evolutionarily conserved role for the aryl hydrocarbon receptor in the regulation of movement. *PLoS Genet.* **2014**, *10*, e1004673. [\[CrossRef\]](#) [\[PubMed\]](#)
24. Houtkooper, R.H.; Mouchiroud, L.; Ryu, D.; Moullan, N.; Katsyuba, E.; Knott, G.; Williams, R.W.; Auwerx, J. Mitonuclear protein imbalance as a conserved longevity mechanism. *Nature* **2013**, *497*, 451–457. [\[CrossRef\]](#)
25. Neuner, S.M.; Garfinkel, B.P.; Wilmott, L.A.; Ignatowska-Jankowska, B.M.; Citri, A.; Orly, J.; Lu, L.; Overall, R.W.; Mulligan, M.K.; Kempermann, G. Systems genetics identifies Hp1bp3 as a novel modulator of cognitive aging. *Neurobiol. Aging* **2016**, *46*, 58–67. [\[CrossRef\]](#)
26. Roy, S.; Sleiman, M.B.; Jha, P.; Williams, E.G.; Ingels, J.F.; Chapman, C.J.; McCarty, M.S.; Ziebarth, J.D.; Hook, M.; Sun, A. Gene-by-environment modulation of lifespan and weight gain in the murine BXD family. *Nat. Metab.* **2021**, *3*, 1217–1227. [\[CrossRef\]](#)
27. Sandoval-Sierra, J.V.; Helbing, A.H.B.; Williams, E.G.; Ashbrook, D.G.; Roy, S.; Williams, R.W.; Mozhui, K. Body weight and high-fat diet are associated with epigenetic aging in female members of the BXD murine family. *Aging Cell.* **2020**, *19*, e13207. [\[CrossRef\]](#)
28. Williams, E.G.; Pfister, N.; Roy, S.; Statzer, C.; Ingels, J.; Bohl, C.; Hasan, M.; Čuklina, J.; Bühlmann, P.; Zamboni, N.; et al. Multiomic profiling of the liver across diets and age in a diverse mouse population. *Cell Syst.* **2022**, *13*, 43–57.e6. [\[CrossRef\]](#)
29. Neuner, S.M.; Heuer, S.E.; Huentelman, M.J.; O'Connell, K.M.S.; Kaczorowski, C.C. Harnessing Genetic Complexity to Enhance Translatability of Alzheimer's Disease Mouse Models: A Path toward Precision Medicine. *Neuron* **2019**, *101*, 399–411.e5. [\[CrossRef\]](#)
30. Neuner, S.M.; Heuer, S.E.; Zhang, J.-G.; Philip, V.M.; Kaczorowski, C.C. Identification of Pre-symptomatic Gene Signatures That Predict Resilience to Cognitive Decline in the Genetically Diverse AD-BXD Model. *Front. Genet.* **2019**, *10*, 35. [\[CrossRef\]](#)
31. Neuner, S.M.; Wilmott, L.A.; Hoffmann, B.R.; Mozhui, K.; Kaczorowski, C.C. Hippocampal proteomics defines pathways associated with memory decline and resilience in normal aging and Alzheimer's disease mouse models. *Behav. Brain Res.* **2017**, *322*, 288–298. [\[CrossRef\]](#) [\[PubMed\]](#)
32. O'Connell, K.M.S.; Ouellette, A.R.; Neuner, S.M.; Dunn, A.R.; Kaczorowski, C.C. Genetic background modifies CNS-mediated sensorimotor decline in the AD-BXD mouse model of genetic diversity in Alzheimer's disease. *Genes Brain Behav.* **2019**, *18*, e12603. [\[CrossRef\]](#) [\[PubMed\]](#)
33. Rosen, G.D.; Pung, C.J.; Owens, C.B.; Caplow, J.; Kim, H.; Mozhui, K.; Lu, L.; Williams, R.W. Genetic modulation of striatal volume by loci on Chrs 6 and 17 in BXD recombinant inbred mice. *Genes Brain Behav.* **2009**, *8*, 296–308. [\[CrossRef\]](#) [\[PubMed\]](#)
34. McKnite, A.M.; Perez-Munoz, M.E.; Lu, L.; Williams, E.G.; Brewer, S.; Andreux, P.A.; Bastiaansen, J.W.M.; Wang, X.; Kachman, S.D.; Auwerx, J. Murine gut microbiota is defined by host genetics and modulates variation of metabolic traits. *PLoS ONE* **2012**, *7*, e3919. [\[CrossRef\]](#)
35. Taylor, B.A.; Heiniger, H.J.; Meier, H. Genetic analysis of resistance to cadmium-induced testicular damage in mice. *Proceedings of the Society for Experimental Biology and Medicine. Soc. Exp. Biol. Med.* **1973**, *143*, 629–633. [\[CrossRef\]](#) [\[PubMed\]](#)
36. Taylor, B.A.; Wnek, C.; Kotlus, B.S.; Roemer, N.; MacTaggart, T.; Phillips, S.J. Genotyping new BXD recombinant inbred mouse strains and comparison of BXD and consensus maps. *Mamm. Genome* **1999**, *10*, 335–348. [\[CrossRef\]](#)
37. Peirce, J.L.; Lu, L.; Gu, J.; Silver, L.M.; Williams, R.W. A new set of BXD recombinant inbred lines from advanced intercross populations in mice. *BMC Genet.* **2004**, *5*, 7. [\[CrossRef\]](#)
38. Wang, J.; Williams, R.W.; Manly, K.F. WebQTL: Web-based complex trait analysis. *Neuroinformatics* **2003**, *1*, 299–308. [\[CrossRef\]](#)
39. Philip, V.M.; Duvvuru, S.; Gomero, B.; Ansah, T.A.; Blaha, C.D.; Cook, M.N.; Hamre, K.M.; Lariviere, W.R.; Matthews, D.B.; Mittleman, G. High-throughput behavioral phenotyping in the expanded panel of BXD recombinant inbred strains. *Genes Brain Behav.* **2010**, *9*, 129–159. [\[CrossRef\]](#)

40. Broman, K.W.; Gatti, D.M.; Simecek, P.; Furlotte, N.A.; Prins, P.; Sen, S.; Yandell, B.S.; Churchill, G.A. R/qt12: Software for Mapping Quantitative Trait Loci with High-Dimensional Data and Multiparent Populations. *Genetics* **2019**, *211*, 495–502. [[CrossRef](#)]
41. Manichaikul, A.; Dupuis, J.; Sen, S.; Broman, K.W. Poor Performance of Bootstrap Confidence Intervals for the Location of a Quantitative Trait Locus. *Genetics* **2006**, *174*, 481–489. [[CrossRef](#)] [[PubMed](#)]
42. Liao, Y.; Wang, J.; Jaehnig, E.J.; Shi, Z.; Zhang, B. WebGestalt 2019: Gene set analysis toolkit with revamped UIs and APIs. *Nucleic Acids Res.* **2019**, *47*, W199–W205. [[CrossRef](#)] [[PubMed](#)]
43. Wang, J.; Duncan, D.; Shi, Z.; Zhang, B. WEB-based GEne SeT AnaLysis Toolkit (WebGestalt): Update 2013. *Nucleic Acids Res.* **2013**, *41*, W77–W83. [[CrossRef](#)] [[PubMed](#)]
44. Wang, J.; Vasaikar, S.; Shi, Z.; Greer, M.; Zhang, B. WebGestalt 2017: A more comprehensive, powerful, flexible and interactive gene set enrichment analysis toolkit. *Nucleic Acids Res.* **2017**, *45*, W130–W137. [[CrossRef](#)]
45. Zhang, B.; Kirov, S.; Snoddy, J. WebGestalt: An integrated system for exploring gene sets in various biological contexts. *Nucleic Acids Res.* **2005**, *33*, W741–W748. [[CrossRef](#)]
46. McLaren, W.; Gil, L.; Hunt, S.E.; Riat, H.S.; Ritchie, G.R.S.; Thormann, A.; Flicek, P.; Cunningham, F. The Ensembl variant effect predictor. *Genome Biol.* **2016**, *17*, 122. [[CrossRef](#)]
47. Sim, N.-L.; Kumar, P.; Hu, J.; Henikoff, S.; Schneider, G.; Ng, P.C. SIFT web server: Predicting effects of amino acid substitutions on proteins. *Nucleic Acids Res.* **2012**, *40*, W452–W457. [[CrossRef](#)]
48. Ng, P.C.; Henikoff, S. SIFT: Predicting amino acid changes that affect protein function. *Nucleic Acids Res.* **2003**, *31*, 3812–3814. [[CrossRef](#)]
49. Eddy, S.R. Where did the BLOSUM62 alignment score matrix come from? *Nat. Biotechnol.* **2004**, *22*, 1035–1036. [[CrossRef](#)]
50. Watanabe, K.; Stringer, S.; Frei, O.; Umičević Mirkov, M.; de Leeuw, C.; Polderman, T.J.C.; van der Sluis, S.; Andreassen, O.A.; Neale, B.M.; Posthuma, D. A global overview of pleiotropy and genetic architecture in complex traits. *Nat. Genet.* **2019**, *51*, 1339–1348. [[CrossRef](#)]
51. Haley, C.; Knott, S. A simple regression method for mapping quantitative trait loci in line crosses using flanking markers. *Heredity* **1992**, *69*, 315–324. [[CrossRef](#)] [[PubMed](#)]
52. Eppig, J.T. Mouse genome informatics (MGI) resource: Genetic, genomic, and biological knowledgebase for the laboratory mouse. *ILAR J.* **2017**, *58*, 17–41. [[CrossRef](#)] [[PubMed](#)]
53. Bennett, B.; Markel, P.D.; Beeson, M.A.; Gordon, L.G.; Johnson, T.E. Mapping quantitative trait loci for ethanol-induced anesthesia in LSxSS recombinant inbred and F2 mice: Methodology and results. *Alcohol Alcohol.* **1994**, *2*, 79–86.
54. Le Roy, I.; Perez-Diaz, F.; Cherfouh, A.; Roubertoux, P.L. Preweanling sensorial and motor development in laboratory mice: Quantitative trait loci mapping. *Dev. Psychobiol.* **1999**, *34*, 139–158. [[CrossRef](#)]
55. Nakamura, K.; Xiu, Y.; Ohtsui, M.; Sugita, G.; Abe, M.; Ohtsui, N.; Hamano, Y.; Jiang, Y.; Takahashi, N.; Shirai, T. Genetic dissection of anxiety in autoimmune disease. *Hum. Mol. Genet.* **2003**, *12*, 1079–1086. [[CrossRef](#)]
56. Håvik, B.; Degenhardt, F.A.; Johansson, S.; Fernandes, C.P.D.; Hinney, A.; Scherag, A.; Lybæk, H.; Djurovic, S.; Christoforou, A.; Erslund, K.M. DCLK1 variants are associated across schizophrenia and attention deficit/hyperactivity disorder. *PLoS ONE* **2012**, *7*, e35424. [[CrossRef](#)]
57. Nair, H.K.; Hain, H.; Quock, R.M.; Philip, V.M.; Chesler, E.J.; Belknap, J.K.; Lariviere, W.R. Genomic loci and candidate genes underlying inflammatory nociception. *Pain* **2011**, *152*, 599–606. [[CrossRef](#)]
58. Riccio, A.; Li, Y.; Tsvetkov, E.; Gapon, S.; Yao, G.L.; Smith, K.S.; Engin, E.; Rudolph, U.; Bolshakov, V.Y.; Clapham, D.E. Decreased anxiety-like behavior and Gαq/11-dependent responses in the amygdala of mice lacking TRPC4 channels. *J. Neurosci.* **2014**, *34*, 3653–3667. [[CrossRef](#)]
59. Mardones, M.D.; Andaur, G.A.; Varas-Godoy, M.; Henriquez, J.F.; Salech, F.; Behrens, M.I.; Couve, A.; Inestrosa, N.C.; Varela-Nallar, L. Frizzled-1 receptor regulates adult hippocampal neurogenesis. *Mol. Brain* **2016**, *9*, 29. [[CrossRef](#)]
60. Barth, A.; Bilkei-Gorzo, A.; Drews, E.; Otte, D.M.; Diaz-Lacava, A.; Varadarajulu, J.; Turck, C.W.; Wienker, T.F.; Zimmer, A. Analysis of quantitative trait loci in mice suggests a role of Enoph1 in stress reactivity. *J. Neurochem.* **2014**, *128*, 807–817. [[CrossRef](#)]
61. Mikasa, M.; Kanai, K.; Li, Y.; Yoshino, H.; Mogushi, K.; Hayashida, A.; Ikeda, A.; Kawajiri, S.; Okuma, Y.; Kashiwara, K. COQ2 variants in Parkinson's disease and multiple system atrophy. *J. Neural Transm.* **2018**, *125*, 937–944. [[CrossRef](#)] [[PubMed](#)]
62. Funato, H.; Miyoshi, C.; Fujiyama, T.; Kanda, T.; Sato, M.; Wang, Z.; Ma, J.; Nakane, S.; Tomita, J.; Ikkyu, A. Forward-genetics analysis of sleep in randomly mutagenized mice. *Nature* **2016**, *539*, 378–383. [[CrossRef](#)] [[PubMed](#)]
63. Takayanagi, Y.; Fujita, E.; Yu, Z.; Yamagata, T.; Momoi, M.Y.; Momoi, T.; Onaka, T. Impairment of social and emotional behaviors in Cadm1-knockout mice. *Biochem. Biophys. Res. Commun.* **2010**, *396*, 703–708. [[CrossRef](#)] [[PubMed](#)]
64. Sarowar, T.; Grabrucker, S.; Föhr, K.; Mangus, K.; Eckert, M.; Bockmann, J.; Boeckers, T.M.; Grabrucker, A.M. Enlarged dendritic spines and pronounced neophobia in mice lacking the PSD protein RICH2. *Mol. Brain* **2016**, *9*, 28. [[CrossRef](#)] [[PubMed](#)]
65. Matsumoto, Y.; Katayama, K.; Okamoto, T.; Yamada, K.; Takashima, N.; Nagao, S.; Aruga, J. Impaired auditory-vestibular functions and behavioral abnormalities of Slitrk6-deficient mice. *PLoS ONE* **2011**, *6*, e16497. [[CrossRef](#)] [[PubMed](#)]
66. Van Dam, S.; Cordeiro, R.; Craig, T.; van Dam, J.; Wood, S.H.; de Magalhães, J.P. GeneFriends: An online co-expression analysis tool to identify novel gene targets for aging and complex diseases. *BMC Genom.* **2012**, *13*, 535. [[CrossRef](#)]
67. Van Dam, S.; Craig, T.; de Magalhães, J.P. GeneFriends: A human RNA-seq-based gene and transcript co-expression database. *Nucleic Acids Res.* **2015**, *43*, D1124–D1132. [[CrossRef](#)]

68. Wang, J.C.; Foroud, T.; Hinrichs, A.L.; Le, N.X.H.; Bertelsen, S.; Budde, J.P.; Harari, O.; Koller, D.L.; Wetherill, L.; Agrawal, A. A genome-wide association study of alcohol-dependence symptom counts in extended pedigrees identifies C15orf53. *Mol. Psychiatry* **2013**, *18*, 1218–1224. [\[CrossRef\]](#)
69. Howard, D.M.; Adams, M.J.; Clarke, T.-K.; Hafferty, J.D.; Gibson, J.; Shirali, M.; Coleman, J.R.I.; Hagenaars, S.P.; Ward, J.; Wigmore, E.M. Genome-wide meta-analysis of depression identifies 102 independent variants and highlights the importance of the prefrontal brain regions. *Nat. Neurosci.* **2019**, *22*, 343–352. [\[CrossRef\]](#)
70. Okbay, A.; Baselmans, B.M.L.; De Neve, J.-E.; Turley, P.; Nivard, M.G.; Fontana, M.A.; Meddens, S.F.W.; Linnér, R.K.; Rietveld, C.A.; Derringer, J. Genetic variants associated with subjective well-being, depressive symptoms, and neuroticism identified through genome-wide analyses. *Nat. Genet.* **2016**, *48*, 624–633. [\[CrossRef\]](#)
71. Ripke, S.; Wray, N.R.; Lewis, C.M.; Hamilton, S.P.; Weissman, M.M.; Breen, G.; Byrne, E.M.; Blackwood, D.H.; Boomsma, D.I.; Cichon, S. A mega-analysis of genome-wide association studies for major depressive disorder. *Mol. Psychiatry* **2013**, *18*, 497–511. [\[PubMed\]](#)
72. Day, F.R.; Ong, K.K.; Perry, J.R.B. Elucidating the genetic basis of social interaction and isolation. *Nat. Commun.* **2018**, *9*, 2457. [\[CrossRef\]](#) [\[PubMed\]](#)
73. Jones, S.E.; Tyrrell, J.; Wood, A.R.; Beaumont, R.N.; Ruth, K.S.; Tuke, M.A.; Yaghootkar, H.; Hu, Y.; Teder-Laving, M.; Hayward, C. Genome-Wide Association Analyses in 128,266 Individuals Identifies New Morningness and Sleep Duration Loci. *PLoS Genet.* **2016**, *12*, e1006125. [\[CrossRef\]](#) [\[PubMed\]](#)
74. Schizophrenia Working Group of the Psychiatric Genomics Consortium. Biological insights from 108 schizophrenia-associated genetic loci. *Nature* **2014**, *511*, 421–427. [\[CrossRef\]](#) [\[PubMed\]](#)
75. Bipolar Disorder and Schizophrenia Working Group of the Psychiatric Genomics Consortium & Bipolar Disorder and Schizophrenia Working Group of the Psychiatric Genomics Consortium. Genomic dissection of bipolar disorder and schizophrenia, including 28 subphenotypes. *Cell* **2018**, *173*, 1705–1715.e16. [\[CrossRef\]](#)
76. Fung, H.-C.; Scholz, S.; Matarin, M.; Simón-Sánchez, J.; Hernandez, D.; Britton, A.; Gibbs, J.R.; Langefeld, C.; Stiegert, M.L.; Schymick, J. Genome-wide genotyping in Parkinson's disease and neurologically normal controls: First stage analysis and public release of data. *Lancet Neurol.* **2006**, *5*, 911–916. [\[CrossRef\]](#)
77. Proenca, C.C.; Gao, K.P.; Shmelkov, S.V.; Rafii, S.; Lee, F.S. Slitrks as emerging candidate genes involved in neuropsychiatric disorders. *Trends Neurosci.* **2011**, *34*, 143–153. [\[CrossRef\]](#)
78. Beaubien, F.; Cloutier, J.-F. Differential expression of Slitrk family members in the mouse nervous system. *Dev. Dyn.* **2009**, *238*, 3285–3296. [\[CrossRef\]](#)
79. Jin, J.; Liu, L.; Chen, W.; Gao, Q.; Li, H.; Wang, Y.; Qian, Q. The Implicated Roles of Cell Adhesion Molecule 1 (CADM1) Gene and Altered Prefrontal Neuronal Activity in Attention-Deficit/Hyperactivity Disorder: A “Gene-Brain-Behavior Relationship”? *Front. Genet.* **2019**, *10*, 882. [\[CrossRef\]](#)
80. Bou Khalil, R.; Khoury, E.; Richa, S. The Comorbidity of Fibromyalgia Syndrome and Attention Deficit and Hyperactivity Disorder from a Pathogenic Perspective. *Pain Med.* **2018**, *19*, 1705–1709. [\[CrossRef\]](#)
81. Treister, R.; Eisenberg, E.; Demeter, N.; Pud, D. Alterations in pain response are partially reversed by methylphenidate (Ritalin) in adults with attention deficit hyperactivity disorder (ADHD). *Pain Pract.* **2015**, *15*, 4–11. [\[CrossRef\]](#) [\[PubMed\]](#)
82. Stray, L.L.; Kristensen, Ø.; Lomeland, M.; Skorstad, M.; Stray, T.; Tønnessen, F.E. Motor regulation problems and pain in adults diagnosed with ADHD. *Behav. Brain Funct.* **2013**, *9*, 18. [\[CrossRef\]](#) [\[PubMed\]](#)
83. Van Breda, S.G.J.; Claessen, S.M.H.; van Herwijnen, M.; Theunissen, D.H.J.; Jennen, D.G.J.; de Kok, T.M.C.M.; Kleinjans, J.C.S. Integrative omics data analyses of repeated dose toxicity of valproic acid in vitro reveal new mechanisms of steatosis induction. *Toxicology* **2018**, *393*, 160–170. [\[CrossRef\]](#)
84. Schulpen, S.H.W.; Pennings, J.L.A.; Piersma, A.H. Gene expression regulation and pathway analysis after valproic acid and carbamazepine exposure in a human embryonic stem cell based neuro-developmental toxicity assay. *Toxicol. Sci.* **2015**, *146*, 311–320. [\[CrossRef\]](#) [\[PubMed\]](#)
85. Rempel, E.; Hoelting, L.; Waldmann, T.; Balmer, N.V.; Schildknecht, S.; Grinberg, M.; Das Gaspar, J.A.; Shinde, V.; Stöber, R.; Marchan, R. A transcriptome-based classifier to identify developmental toxicants by stem cell testing: Design, validation and optimization for histone deacetylase inhibitors. *Arch. Toxicol.* **2015**, *89*, 1599–1618. [\[CrossRef\]](#) [\[PubMed\]](#)
86. Reuterswärd, P.; Bergström, S.; Orikiiriza, J.; Lindquist, E.; Bergström, S.; Andersson Svahn, H.; Ayoglu, B.; Uhlén, M.; Wahlgren, M.; Normark, J. Levels of human proteins in plasma associated with acute paediatric malaria. *Malar. J.* **2018**, *17*, 426. [\[CrossRef\]](#)